Atomistic Structure of Band-Tail States in Amorphous Silicon

Jianjun Dong and D. A. Drabold

*Department of Physics and Astronomy, Condensed Matter and Surface Science Program, Ohio University,
Athens, Ohio 45701-2979*
(Received 31 July 1997)

We compute accurate approximations of the electronic states near the gap in a very large and realistic model of *a*-Si. The spatial structure of the states is computed explicitly and discussed. The character of the local to the extended (Anderson) transition in amorphous Si is described. The density of states, the conductivity, and doping are discussed. [S0031-9007(98)05414-3]

The nature of the band-tail states in amorphous semiconductors is of both fundamental and applied interest. Since the seminal work of Anderson [1] it has been known that disorder induces localization of electron states. The detailed understanding of this has been a field of tremendous activity in condensed matter theory. In the parlance of amorphous semiconductors, the nature of the electron localization is determined by the microscopic structure of the band-tail and midgap eigenstates and the dependence of this structure on the energy of the state. In this Letter, we report the first explicit microscopic calculations of the band-tail states using a very large and realistic 4096 atom model of *a*-Si (a cube about 43 Å on a side), generated by Djordjevic, Thorpe, and Wooten [2]. A related calculation for amorphous diamond has been published recently [3]. This paper goes well beyond related earlier work [4] on 216 or fewer atom cells, which accurately modeled deep gap states, but was limited in showing their ability to model *tail* states.

A localized-to-extended [1,5] transition occurs near both the valence and conduction band tails in *a*-Si, since midgap states are bound to be Anderson localized in a realistic model of *a*-Si and, likewise, states well into the valence or conduction bands (beyond the mobility edges) are extended. While this picture is certainly valid, it is also qualitative, and details, such as the exact nature of the mobility edge, are still controversial. Within finite-size limitations of our model, we indicate qualitative features of the transition that are robust and salient to real *a*-Si and that we suspect are relevant to any topologically disordered insulator.

For applications, and for any transport experiments on *a*-Si [6], the gap and band-tail states are of interest. For example, in a lightly boron doped (*p*-type) sample of *a*-Si:H, one can expect that states much like the ones we report near the valence edge will be responsible for the conduction [7]. Any atomistic approach to computing conductivity and transport properties must start from calculations of the electron states near the Fermi level as we compute for a very large cell of *a*-Si for the first time in this paper.

The approximations of this paper are as follows: (1) An orthogonal tight-binding Hamiltonian [8] with one *s*

and three *p* basis functions per site and (2) the 4096 atom supercell model of *a*-Si proposed in Ref. [2]. The tight-binding model is an imperfect means of modeling electronic structure, but calculations [4] demonstrate that the qualitative features of the localization of electronic states due to disorder and their qualitative placement compares well to experiment or to more sophisticated theory [9]. The supercell model of Djordjevic and coworkers has been discussed in detail in the literature [2]. It has a pair distribution function, bond angle distribution, and, as we will show, electronic properties in rather good *and uniform* agreement with experiment. It has no three-coordinated (dangling bond) sites. In addition, we have relaxed a 512 atom model constructed analogously [2] to the 4096 atom cell studied here with local basis local density approximation (LDA) methods [9], and only minor changes were noted from the original coordinates.

Since the Hamiltonian we are using involves four basis functions per atom, the dimension of the Hamiltonian matrix **H** is $N = 4 \times 4096 = 16\,384$. This is too large to exactly diagonalize with traditional methods [10]. Since the matrix is sparse (because the range of the tight-binding matrix elements is small), a small subset of the complete set of eigenstates of the matrix can be computed essentially exactly with a Lanczos [10] technique. We use our maximum entropy method [11] to compute the global density of states.

We estimate the electrical conductivity of the model, using the Kubo formula [12] for the ac conductivity,

$$\sigma(\omega) = \frac{2\pi e^2}{3m^2 \Omega \omega} \sum_{i,k} [f_i - f_k] |M_{i,k}|^2 \times \delta(E_k - E_i - \hbar\omega), \quad (1)$$

where $M_{i,k} = \langle \psi_i | \hat{\mathcal{P}} | \psi_k \rangle$ is the momentum operator matrix element between eigenstates ψ_i and ψ_k, Ω is the cell volume, and E_i is the energy of state i. f_i is the Fermi-Dirac distribution function evaluated at energy E_i. By inspection of the Kubo formula, it is clear that the localization of the states overlap (and momentum matrix elements), and proximity in energy to each other and to the Fermi level are primary determinants of the dc conductivity. Thermal (electron-phonon) effects are also quite important at $T > 0$; we discuss this elsewhere [13].

The density of states for **H** is reproduced in Fig. 1(a): the global structure of the density of states is shown in the inset. The valence edge shows more tailing than the conduction edge: this is consistent with experiments [14] and theory [15] which show that the valence tail is primarily due to structural disorder, while the conduction tail is much more sensitive to temperature and originates in thermal disorder. Since this is a zero temperature calculation, the relatively greater width of the valence tailing is to be expected. The solid curve of Fig. 1(a) is the maximum entropy fit to the density of states, and is quite exponential, similar to what we observed in amorphous diamond [3]. The decay parameter E_0 [such that density of states $\rho(E) \sim \exp(-E/E_0)$] is 190 meV. In earlier calculations on 216 or fewer atom cells, there are simply too few states to get a reasonable sampling of the band-tail energy range [4,13].

Next, we computed 500 midgap and band-tail electronic eigenstates in the energy range between -0.5 and
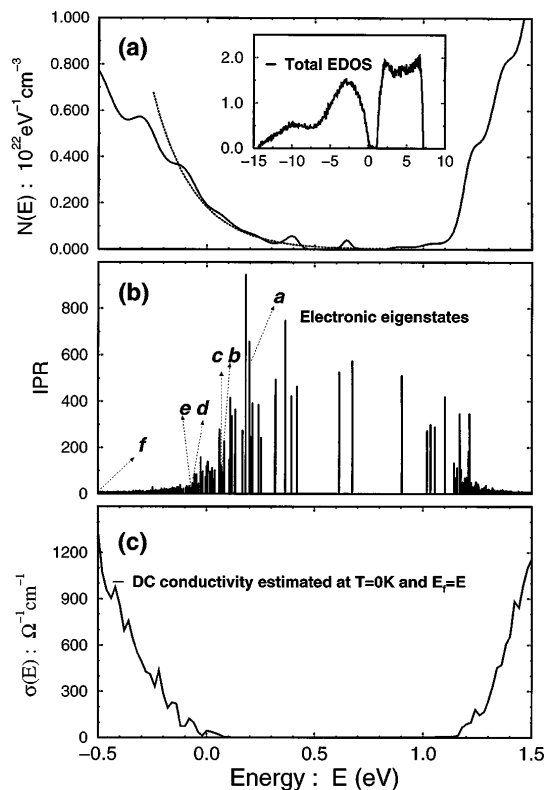

FIG. 1. Electronic states in the band-gap region: (a) Electronic density of states (DOS) computed by the maximum-entropy technique [11]. The total DOS is condensed in the graph shown in the inset. 400 moments and 50 random vectors were used (Ref. [11]). The valence band tail is approximately exponential with width of 190 meV as estimated with the fitting function (dashed line). (b) Energies and localization [from inverse participation ratio—IPR (see text)] of gap states from Lanczos calculation. Large IPR implies more spatial localization. The letters illustrate the location in energy of the eigenstates depicted in Fig. 2. (c) The estimated dc conductivity as a function of doping (location of the Fermi level) computed with the Kubo formula [Eq. (1)].

1.5 eV essentially exactly using the Lanczos [10] scheme. The position and localization of the individual states are reported in Fig. 1(b). Each spike indicates an energy eigenvalue, and the height of the spike is the localization from the inverse participation ratio (IPR): $I(\psi_n) = N \sum_{i=1}^{N} a_{ni}^4 / (\sum_{i=1}^{N} a_{ni}^2)^2$, where $\psi_n = \sum_{i=1}^{N} a_{ni} \phi_i$ is the nth eigenvector and ϕ_i is one of the N orthogonal (tight-binding) basis orbitals. The IPR for ideally extended states is near 1.0, and an ideally localized state (on one basis orbital) would yield $I = N$. Figure 1(b) shows a smooth falloff in IPR as energy (doping) changes from midgap (say, near 0.5 eV) into the valence tail (near 0.0 eV). If the exact position of the eigenvalues from Fig. 1(b) are fit to an exponential form for the tail [dashed curve in Fig. 1(a)], we get almost exactly the same tail as from maximum entropy. In Fig. 1(c), we estimate the dc conductivity using the Kubo formula [12], where in this plot, the abscissa indicates the position of Fermi level and the predicted conductivity from the states discussed in Fig. 1(b). We note that (1) the midgap states are incapable of carrying current since they are localized and sparse in the energy gap, (2) if the states become dense (and extended) enough, a nonzero conductivity is obtained when the model is doped to a Fermi level near $E = 0$, and (3) the conductivity rises *smoothly* with increasing p-doping. There is no signature in this work of an abrupt mobility edge [5]. To estimate the dc conductivity, we average $\sigma(\omega)$ from the Kubo formula [12] in a small band of width $\delta\omega = 0.02$ eV about $\omega = 0$. We admit that for the energy region around 0.1 eV where the states are sparse, the result is somewhat sensitive to the choice of $\delta\omega$ due to finite-size artifacts. So it is hard to pin the *exact* location of the mobility edges in our calculation. However, the basic structure of the curve is very plausible, and it would seem that the mobility gap extends from 0.0 to about 1.2 eV.

To study the spatial structure of electron states and the qualitative nature of the local-to-extended transition, we "visualize" states by assigning different colors to every atom according to the "charge" associated with the atom site for a given eigenstate. In Fig. 2, we choose six typical valence states. The position of these states are also cross labeled as $a-f$ in Fig. 1(b). For the effect of visualization, only 75% charge in each state is shown (those atom sites contributing less charge density are omitted). Changes in color thresholds modify the detailed appearance, but the features we discuss are robust to sensible changes in the visualization. Figure 2(a) is a typical exponentially localized state where the charge is confined to a small cluster of atoms near a major structural distortion (bond angles severely deviating from tetrahedral bonding). The size of the cluster increases as the energy is tuned from midgap toward valence band (it is not perfectly monotonic). For energies deeper into the valence band ($E < 0.1$ eV), the eigenstate "proliferates" into a form consisting of several small clusters. At the beginning of this phase, an energy eigenstate is a superposition
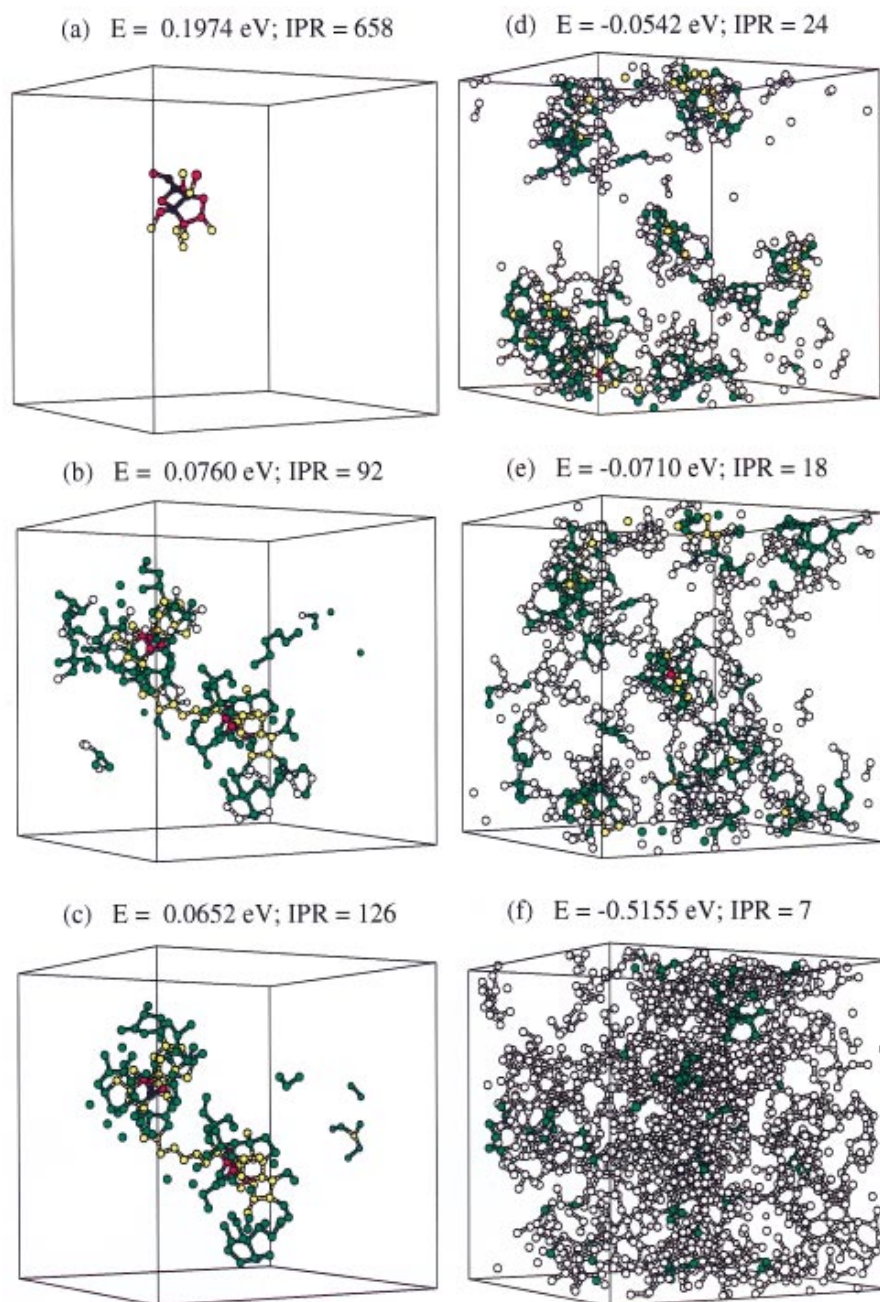
FIG 2(color).   Spatial character of the local-to-extended transition: energy eigenstates. For a given state of energy E with position as indicated in Fig. 1(b), IPR is the inverse participation ratio (see text), and electron charge density is depicted according to the color. Each atom shown is colored according to the fraction of total charge: black ($>1/16$), red ($>1/64$), yellow ($>1/256$), green ($>1/1024$), and white ($<1/1024$, such that at least 75% of the total charge is shown). The electronic states evolve from the tightly localized (midgap) states (a) to weakly coupled "cluster" states (b) and (c), to fragmented multiclusters states (d) and (e), and finally to extended valence states (f).

of two clusters weakly overlapping each other in real space. This could be understood with perturbation theory: two nearly energy degenerate localized clusters weakly overlapping each other will admix to form two new states. One (of several) examples supporting this are two states $|\psi_b\rangle$ and $|\psi_c\rangle$, split by a small energy (10 meV), depicted in Figs. 2(b) and 2(c), which appear to be built from two weakly overlapping clusters. By computing $|\pm\rangle = |\psi_b\rangle \pm |\psi_c\rangle$, we obtain new states much more localized than $|\psi_b\rangle$ or $|\psi_c\rangle$ and resembling the upper ($+$)

or lower ($-$) clusters in Figs. 2(b) and 2(c). The states $|\pm\rangle$ are nearly localized eigenstates of **H**, since $|\psi_b\rangle$ and $|\psi_c\rangle$ are almost degenerate. For energies near the mobility gap we conjecture the existence of cluster states $|\alpha\rangle$; exact localized eigenstates due to a given *isolated* distortion. The states of Fig. 2, especially Figs. 2(b) and 2(c) are interpreted as mixtures of overlapping, nearly degenerate cluster states $|\alpha\rangle$. $|\pm\rangle$ are *approximations* to the $|\alpha\rangle$, since $|\pm\rangle$ are not ideally isolated from each other in this model with its realistic distribution of defects. This

is reasonable, since major defects induce local (cluster) states [4]: more common, milder defects induce less localized cluster states which overlap in realistic models of *a*-Si, and are therefore not isolated, but whose existence can be inferred from the eigenstates (perturbatively, superpositions of the cluster states). We next displaced one atom with largest localization from the upper cluster of either Fig. 2(b) or Fig. 2(c), 0.09 Å and recomputed eigenstates. A cluster similar to the lower cluster was a new eigenstate with an energy between original states $|\psi_b\rangle$ and $|\psi_c\rangle$. The displacement pushed $|+\rangle$ "off resonance" with $|-\rangle$, as our model would predict.

We note that the dc conductivity plotted in Fig. 1(c) begins to rise from zero just at the energy where the electronic states begin to proliferate into multiple clusters. For deeper valence states, eigenfunctions consist of three or more clusters and become "quasiextended." Now states are more complicated and could not easily be decomposed into primitive localized clusters. Still, for a small band-tail energy range, we find that the same small clusters appear in different eigenstates. This means that the eigenstates are still built by mixing several clusters of similar energies. In Figs. 2(d)–2(e), the two states contain more than seven clusters each. Of these seven, the two upper-left clusters and the middle one in both are similar. As the energy moves deep into the band, the charge density becomes extended and uniform as shown in Fig. 2(f).

Our qualitative picture of the local to extended transition in *a*-Si, based on our detailed calculations, is the following: As severe distortions are rare, clusters stemming from such distortions are probably isolated from each other and, if isolated, are localized energy eigenstates. For less severe distortion, the probability of occurrence increases, and the size of associated clusters is also larger. Then the chance of finding another cluster of similar energy in the neighborhood increases. As the distortion becomes less severe, two, three, or more clusters could mix together. At some point, clusters can always find "overlapping energy partners," and they mix together to enable electronic connectivity. This state of affairs can be identified with the "mobility edge." In some ways, our model resembles results from classical percolation theory for conductivity [16].

Our "resonant cluster proliferation" model can be roughly formalized in an effective or "coarse grained" Hamiltonian valid in the band-tail and midgap region,

$$\hat{H}_{\text{tail}} = \sum_\alpha E_\alpha |\alpha\rangle\langle\alpha| + \sum_{\alpha\beta(\alpha \neq \beta)} |\alpha\rangle\xi_{\alpha\beta}\langle\beta|, \quad (2)$$

where basis state $|\alpha\rangle$ is a localized cluster (*which will consist of many atoms*). In this representation, the basis functions are localized energy eigenstates with eigenvalue E_α of the Hamiltonian in the absence of other defects with which mixing occurs. $|+\rangle$ and $|-\rangle$ above are close *approximations* to the $|\alpha\rangle$. E_α is determined by the distortion. In real amorphous solids, the cluster states may significantly overlap. $\xi_{\alpha\beta}$ represents the coupling between

clusters $|\alpha\rangle$ and $|\beta\rangle$. In the spirit of Hückel theory [17], we can take $\xi_{\alpha\beta} \sim (E_\alpha + E_\beta)S_{\alpha\beta}/2$ for $S_{\alpha\beta} = \langle\alpha \mid \beta\rangle$. Then, in first order perturbation theory, the formation of eigenstates of **H** from these clusters becomes obvious; the first order correction to the zeroth-order (cluster) state $|\alpha\rangle$ is $\sum_{\beta\neq\alpha} \Gamma_{\alpha\beta}|\beta\rangle$, where $\Gamma_{\alpha\beta} = (E_\alpha + E_\beta)S_{\beta\alpha}/2(E_\alpha - E_\beta)$. The strong mixing for small energy denominators ($E_\alpha \approx E_\beta$) and the role of the overlap are indicated. We will develop this approach further elsewhere [13].

[1] P. W. Anderson, Phys. Rev. **109**, 1492 (1958).

[2] B. R. Djordjevic, M. F. Thorpe, and F. Wooten, Phys. Rev. B **52**, 5685 (1995).

[3] J. Dong and D. A. Drabold, Phys. Rev. B **54**, 10 284 (1996).

[4] R. Biswas *et al.,* Phys. Rev. Lett. **63**, 1491 (1989); J. L. Mercer and M. Y. Chou, Phys. Rev. B **43**, 6768 (1991); C. S. Nichols and K. Winer, Phys. Rev. B **38**, 9850 (1988); for a related Bethe lattice calculation, P. A. Fedders and A. E. Carlsson, Phys. Rev. B **39**, 1134 (1989); D. Allan and J. Joannopoulos, in *Hydrogenated Amorphous Silicon II,* edited by J. Joannopoulos and G. Lucovsky (Springer, Berlin, 1984), p. 5.

[5] N. F. Mott and E. A. Davis, *Electronic Processes in Non-Crystalline Materials* (Clarendon, Oxford, 1979), 2nd ed.

[6] See, for example, G. Adriaenssens, in *Amorphous Insulators and Semiconductors,* edited by M. F. Thorpe and M. I. Mitkova, NATO ASI Series (Kluwer, Dordrecht, 1997), p. 437.

[7] P. A. Fedders and D. A . Drabold, Phys. Rev. B **56**, 1864 (1997).

[8] I. Kwon *et al.,* Phys. Rev. B **49**, 7242 (1994). This Hamiltonian gives an optical gap in *c*-Si of 0.78 eV.

[9] O. F. Sankey and D. J. Niklewski, Phys. Rev. B **40**, 3979 (1989).

[10] G. H. Golub and C. F. Van Loan, *Matrix Computations* (Johns Hopkins University Press, Baltimore, 1983). A sophisticated and convenient implementation of the Lanczos method is due to M. T. Jones and M. L. Patrick, 1989, available from netlib as "lanz."

[11] D. A. Drabold and O. F. Sankey, Phys. Rev. Lett. **70**, 3631 (1993); D. A. Drabold, in *Amorphous Insulators and Semiconductors,* (Ref. [6]), p. 405.

[12] D. J. Thouless, Phys. Rep. **13**, 93 (1974).

[13] J. Dong and D. A. Drabold (unpublished).

[14] S. Aljishi *et al.,* Phys. Rev. Lett. **64**, 2811 (1990).

[15] D. A. Drabold *et al.,* Phys. Rev. Lett. **67**, 2179 (1991).

[16] R. Zallen, *The Physics of Amorphous Solids* (John Wiley & Sons, New York, 1983).

[17] For example, W. Harrison, *Electronic Structure and the Properties of Solids: The Physics of the Chemical Bond* (Freeman, New York, 1980), p. 47.